Supplementary material to the paper:

"Increased impact resistance of cross-country ski poles by improved, simulation assisted composite design"

In Proceedings of the 12th ISEA 2018, Brisbane, Australia, 2018

Martin Granlund[1], Gustav Gräsberg[1], Hana Zrida[1], Martin Fagerström[1]

[1] Department of Industrial and Materials Science, Division of Material and Computational Mechanics, Chalmers University of Technology, SE-41296 Gothenburg, Sweden

1. Introduction

Below follows supplementary materials to the main paper which could not be included due to the maximum number of pages allowed, but which could still be of interest to many readers. In the paper, results from the mechanical and numerical testing of different pole brands are summarised. Considered poles were: *Skigo Race 2.0* (from 2016 and from 2017, denoted *SKIGO1* and *SKIGO2* respectively), *Fischer RCS Carbonlite*, *Fischer RCS Speedmax* and *Swix Triac 2.5*. The purpose of the mechanical tests was both to characterise material properties needed for the simulations, see Section 2 below, and to better understand how the material architecture, e.g. fibre orientation of the different layers (or plies), influence the material response.

Furthermore, numerical finite element models were developed as a tool for simulation driven design process which when fully developed allows for finding an optimal balance between competing requirements on weight, stiffness and strength.

2. Material data for *Skigo Race 2.0* used in the numerical simulations

The test experimental test methods to characterise the properties are described in the main paper and not repeated here. Instead, the results are described more in detail and all material properties used in the FE-modelling are summarised.

From the tensile test, the axial pole stiffness was determined. Using the rule of mixtures, the longitudinal stiffness was then back-calculated to be approx. $E_L = 146{,}1 \pm 4{,}3$ GPa for *SKIGO1* and $E_L = 150{,}5 \pm 10{,}2$ GPa for *SKIGO2*. The shear modulus obtained from the torsional test was determined as $G_{LT} = 4.3 \pm 1.3$ GPa for *SKIGO1* and $G_{LT} = 4{,}7 \pm 0{,}4$ GPa for *SKIGO2*. The low number of specimens gave a rather high scatter in the data, yet sufficient for the simulations. Unfortunately, the adhesive was not strong enough to reach tensile failure of the specimens so this value could not be determined.

From the compression load until failure, the ultimate stress and strain were calculated at the point where the tested specimen were no longer able to support any load. The maximum stress obtained was (616,5±97,1) MPa for *SKIGO1* and (931,0±77,5) MPa for *SKIGO2*. The strain at failure was (0,57±0,01) % and (0,59±0,09) % for *SKIGO1* and *SKIGO2*, respectively.

As can be seen, only a few material parameters were characterised. The remaining properties were estimated from a table in [1] for a material with similar longitudinal stiffness. All the material properties used in the simulations for the CFPR plies are summarised in Table 1 below.

Table 1. Material properties used in the FE-analyses of *SKIGO1* and *SKIGO2. Measured values are marked with *, the rest are estimated from [1].*

	SKIGO1	*SKIGO2*
longitudinal stiffness, E_L^* [GPa]	146.1	150.5
transverse stiffness, E_T [GPa]	9.65	9.65
major Poisson's ratio, υ_{LT}	0.3	0.3
in-plane shear modulus, G_{LT}^* [GPa]	4.3	4.7
transverse shear modulus, $G_{TT'}$ [GPa]	2.15	2.35
tensile strength, longitudinal direction [MPa]	1,314	1,314
compressive strength, longitudinal direction* [MPa]	616.5	931
tensile strength, transverse direction [MPa]	43	43
compressive strength, transverse direction [MPa]	168	168
tensile strength, transverse out-of-plane direction [MPa]	43	43
compressive strength, transverse out-of-plane direction [MPa]	168	168
in-plane shear strength [MPa]	48	48
transverse shear strength [MPa]	48	48

3. Extended results from microscopy study

In the microscope, the layup, the fibre area fraction, the fibre diameters as well as the void content were investigated. For each microscopy analysis, thin samples of the cross-section were cast in epoxy and then polished to a fine surface finish, Fig. 1 shows a polished casting with three cross-sections.

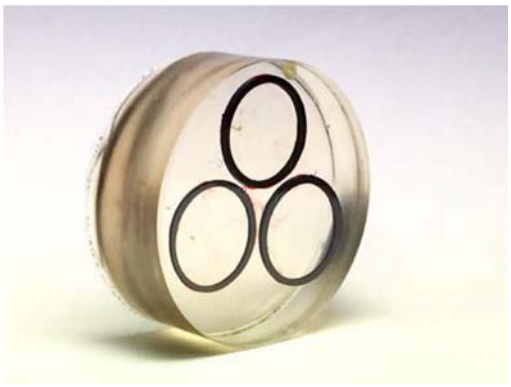

Figure 1. Microscopy samples in epoxy casting.

From the microscopy, the fibre directions can be identified depending on the shape of the fibres cross-section. A circle would be a fibre normal to the cross-sectional surface. Elliptic shapes implies that the fibre is at an angle and the fibres appearing as white lines are parallel with the cross-section surface. Although not exact, off-axis fibre angles (not 0° nor 90°) were estimated based on simple trigonometric relations based on the ration between the major and the minor axis of the ellipses. As can be seen below, it was not always straightforward to determine the exact angle.

3.1. Results from microscopy study of SKIGO1

The lay-up of *SKIGO1* was determined as [45/0_5] from the inside-out, see also Fig. 2 below. The thickness of the inner 45° ply was approx. 65 μm whereas the 0° plies were approx. 170 μm thick except the outer one which was 210 μm thick.

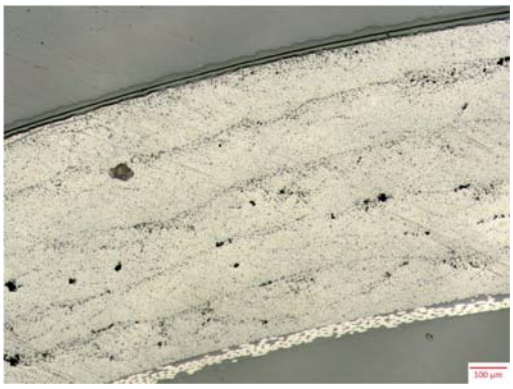

Figure 2. Microscopy image of a *SKIGO1* sample.

3.2. Results from microscopy study of SKIGO2

The lay-up of *SKIGO2* was determined as [**0**/0/90/0/90/**0**/0/90] from the inside-out, see also Fig. 3 below. As can be noted, some of the 0 plies have been made boldface to illustrate that two types of 0° plies were found. Some (the bold) with a fibre diameter of 7.1 μm and a volume fraction of fibres of 55%, and some (non-bold) with a fibre diameter of 5.5 μm with a volume fraction of fibres of 64%. Furthermore, the thickness of the 90° plies were ~25-30 μm whereas the thickness of the 0° plies were in the range of 120-140 μm except for the outer-most ply which was only approximately half as thick.

Figure 3. Microscopy image of a *SKIGO2* sample.

3.3. Results from microscopy study of Fischer RCS Carbonlite

The lay-up of *Fischer RCS Carbonlite* was dominated by 0° plies. However, as can be seen in Fig. 4, on the inside and outside other orientations were identified. The exact angle for these were hard to determine but they seem to be rather close to 90°. Two such layers were found on the inside and one layer on the outside. The thickness of the 0° plies were in average 61.6 μm and the thickness of the nearly 90° oriented plies were 98.9 μm.

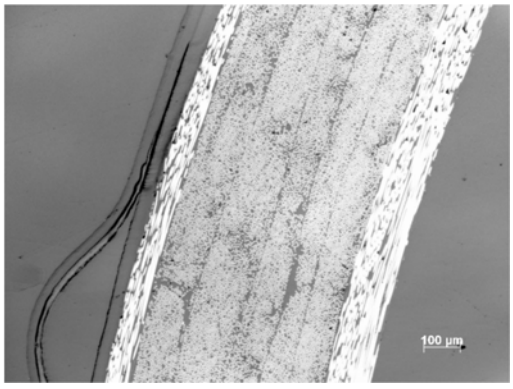

Figure 4. Microscopy image of a *Fischer RCS Carbonlite* sample.

3.4. Results from microscopy study of Fischer RCS Speedmax

The lay-up of *Fischer RCS Speedmax* was dominated by plies with almost 0° orientation. However, as can be seen in Fig. 5, on the inside another orientation was detected. The exact angle for this inner ply was hard to determine but it appears to be rather close to 90°. In the image to the right showing a fracture surface of the same pole, it can be seen that also the (nearly) longitudinal plies has a small offset angle. This suggests that these poles may have been manufactured by filament winding.

The thickness of the almost 90° ply was 122.2 μm and the thickness of the nearly 0° plies were 150.7 μm in average.

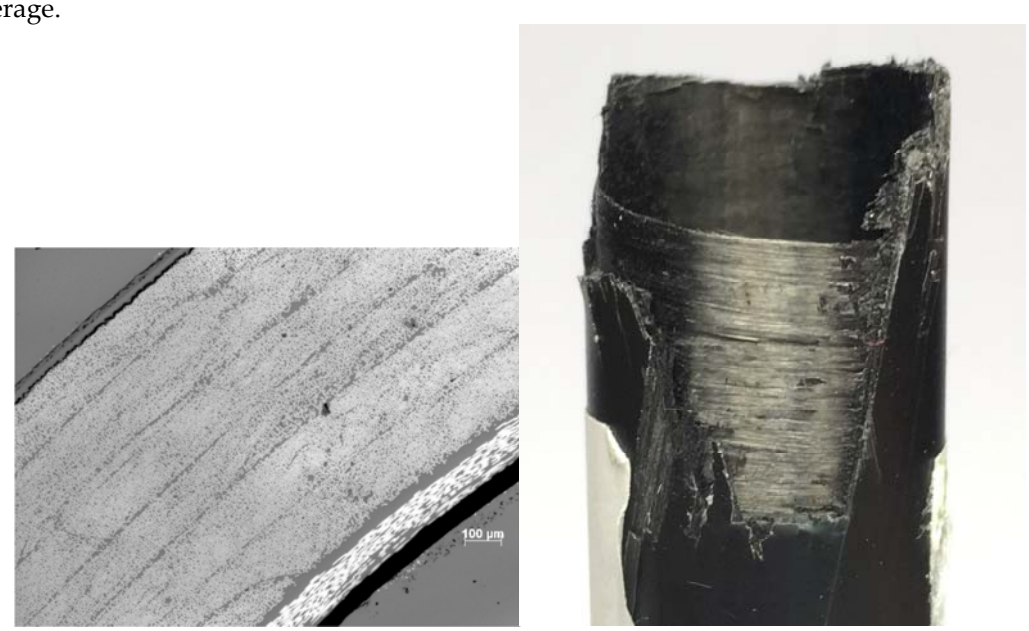

Figure 5. Microscopy images of a *Fischer RCS Speedmax* samples.

3.5. Results from microscopy study of Swix Triac 2.5

The lay-up of the Swix Triac 2.5 ski pole was found to be [45/0_7], see Fig. 36. The thickness of the 45° ply was approximately 70 μm and the thickness of the thickness of the 0° plies were in average approximately 94 μm.

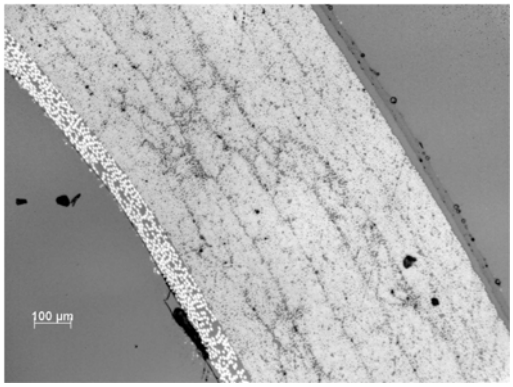

Figure 6. Microscopy image of a *Swix Triac 2.5* sample.

References

1. Agarwal, B.D.; Broutman, L.J.; Chandrashekhara, K. *Analysis and performance of fibre composites*, 3rd ed.; John Wiley and Sons: New Delhi, 2006.